Global Journal of Earth Science and Engineering, 2024, 53-67

Published by Avanti Publishers

Global Journal of Earth Science and Engineering

ISSN (online): 2409-5710

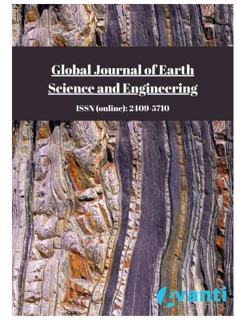

Seismic Background Noise Level and Station Detectability in the Flores Sea

Azmi Khusnani[1,*], Adi Jufriansah[1], Ade Anggraini[2], Ota W. J. Thalo[3] and Konsenius W. Wae[1]

[1]*Physics Education, Faculty of Mathematics and Science Education, Universitas Muhammadiyah Maumere, Maumere 86118, Indonesia*

[2]*Geoscience Research Group, Department of Physics, Faculty of Mathematics and Natural Sciences, Universitas Gadjah Mada, Yogyakarta 55281, Indonesia*

[3]*Fransiskus Xaverius Seda Class III Meteorological Station, Meteorological, Climatological, and Geophysical Agency, Jakarta 3540, Indonesia*

ARTICLE INFO

Article Type: Research Article

Academic Editor: Mohamed EL Hilali

Keywords:
Noise
Flores sea
Earthquake
Seismic background
Probability density function

Timeline:
Received: September 30, 2024
Accepted: December 02, 2024
Published: December 17, 2024

Citation: Khusnani A, Jufriansah A, Anggraini A, Thalo OWJ, Wae KW. Seismic background noise level and station detectability in the Flores Sea. Glob J Earth Sci Eng. 2024; 11: 53-67.

DOI: https://doi.org/10.15377/2409-5710.2024.11.4

*Corresponding Author
Email: husnaniazmi@gmail.com
Tel: +(62) 823 2566 3537

ABSTRACT

The Flores back-arc thrust fissure is a significant contributor to earthquake events in the Flores Sea region, as evidenced by seismic investigations. As part of the endeavor to mitigate earthquake risk, seismic data investigations are necessary due to the high potential for earthquakes in the Flores Sea. Background noise in earthquakes is the term used to describe the micro vibrations that are perpetually produced as a result of natural phenomena, such as ocean waves, wind, or human activities. It is crucial to investigate this cacophony in seismology in order to distinguish the primary earthquake signal. Its spectrum analysis can assist in the identification of land changes and the prediction of tectonic activity. This analysis was conducted by employing the Incorporated Research Institutions for Seismology (IRIS) client function as a fetch data tool and the Modular Utility for Statistical Knowledge Gathering Data browser as a data quality monitoring system to verify the health and reliability of seismic data. The three station sites closest to the Flores Sea are the focus of this research data examination. The study's findings indicate that the recorded data at the station is still dominated by cultural noise, as evidenced by the analysis of the probability density function, power spectral density, and noise spectrograms. Additionally, each station exhibits activity with degrees of probability noise that are both high and variable. These results highlight the need for advanced techniques to filter cultural noise and improve the accuracy of seismic signal interpretation in this region. This analysis contributes to understanding tectonic activity in the Flores Sea and underscores the importance of continuous monitoring for earthquake preparedness and risk reduction.

1. Introduction

A significant disaster in Indonesian history occurred on December 12, 1992, when a massive earthquake with a magnitude of 7.8 struck the northern coastal region of Flores, Indonesia [1-4]. This earthquake was a catastrophic event that resulted in the destruction of over 25,000 buildings and a significant amount of infrastructure, as well as the deaths of over 2000 individuals, the disappearance of over 500 individuals, and the injury of thousands of others [5-8]. Flores Island is situated in an active tectonic region and is a part of the Pacific Ring of Fire, as indicated by geological data [9, 10]. This results in the Flores region being susceptible to tectonic disturbances [11, 12]. The earthquake catalog indicates that the region has experienced earthquakes with a magnitude greater than 7, with three of these occurrences occurring in the Flores Sea in 1992, 1996, 2015, and 2021 [9, 13, 14].

The memory of the devastation remains vivid, despite the passage of more than 30 years. This memory is intensified by the Flores Sea earthquake phenomenon on December 14, 2021, which had a magnitude of 7.3 [14-16]. This necessitates seismic background analysis in the Flores Sea region. The analysis of seismic background analysis can serve as the foundation for probabilistic seismic hazard analysis [17]. It is crucial to conduct this analysis in order to determine the trend of seismic data in the Flores Sea region, which is derived from specific stations. Furthermore, it will furnish information regarding the grade of the seismic data that has been acquired, including noise values [18]. The fundamental capacity to detect seismic signals is significantly influenced by the noise level at the station [19]. Additional findings will determine whether the earthquake phenomenon in the North Sea of Flores is associated with the phenomenon influenced by the Flores back-arc thrust fault. Furthermore, additional research recommends that the seismic context be analyzed using data from mainshocks and aftershocks [18].

One can observe seismic background by analyzing data from seismic stations [20, 21]. The Signal-to-Noise Ratio (SNR) value, which is of paramount significance in the fields of seismology and earthquake monitoring, will be demonstrated in this analysis [22, 23]. The McNamara and Buland analysis method [24] will be employed to evaluate the noise level by calculating the Probability Density Function (PDF). The SNR is determined by the PDF and noise spectrogram, which employ distinct but complementary methodologies [25, 26]. PDF provides a comprehensive overview of the average and extreme noise conditions at a specific location by describing the statistical distribution of noise at various frequencies. This assists in evaluating the potential of a location to generate optimal SNR measurements. However, PSD is a critical instrument for determining SNR by comparing signal energy to noise at a specific frequency, as it quantitatively measures the distribution of noise energy over frequency. Noise spectrograms add a temporal dimension by showing how noise energy changes over time. This lets you find noise fluctuations or the best time to pick up signals with a high signal-to-noise ratio (SNR). A comprehensive evaluation of the quality and reliability of seismic signals can be achieved by combining these three categories of data to perform noise analysis statistically, spectrally, and temporally.

2. Study Area

The high seismic activity in the Flores Sea is a significant concern for geophysical research and disaster mitigation [9], particularly in relation to the detection capability of seismic stations in the region and the level of seismic background noise. The geological conditions of the Flores Sea, the seismic activity that takes place, and the obstacles to seismic measurement and monitoring in this region will be the subject of this study.

2.1. Flores Sea Geological Conditions

The Flores Sea is situated in an active subduction zone, where the Indo-Australian Plate is moving northward and sinking beneath the Eurasian Plate [27-29]. This subduction process results in the formation of a variety of intricate geological features, such as active fissures, ocean trenches, and volcanoes [29, 30]. The Flores Trench, a subduction zone where the deeply buried ocean crust subsides, is one of the primary features that is directly associated with seismic activity [31]. Earthquakes and volcanic eruptions are frequently observed in the vicinity as a result of the extremely high pressure generated by this subduction zone [32]. The Flores Sea is also impacted by lesser local tectonic activities, such as active faults and minor plate movements, in addition to the subduction process [33, 34]. These processes result in crustal deformation, which can induce earthquakes of varying intensity, ranging from minor to major. Consequently, the Flores Sea region is a region that is highly susceptible to earthquakes and other natural disasters.

2.2. Seismic Activity in the Flores Sea

The seismicity of earthquakes in the Flores Sea is quite high, as it is situated at the convergence of two main tectonic plates, which are characterized by substantial tectonic and volcanic earthquake activity [11, 35]. According to the most recent data from the Meteorology, Climatology, and Geophysics Agency (BMKG), the Flores Sea is classified as an area with a high incidence of earthquakes, particularly in the vicinity of the Flores Trench [36, 37]. This region has been the site of numerous significant earthquakes, including those with a Richter scale magnitude exceeding 7.0, which frequently occur along subduction zones [14]. The risk of calamity for coastal communities is frequently elevated by the presence of tsunamis in conjunction with these earthquakes [6, 15]. Furthermore, the Flores Sea experiences substantial volcanic activity, which contributes to the rise in the frequency of non-tectonic earthquakes, which are frequently more intense and shallow [34]. This rise in volcanic activity can result in an increase in seismic noise levels, which complicates the monitoring and analysis of precise seismic data [38].

The potential for earthquakes in the Flores region is attributed to the Flores back-arc thrust fault, shallow and intermediate thrust zones in Timor Through, intermediate depth thrusts, and subduction earthquake zones, as determined by seismic study analysis [9, 13, 39]. This information is substantiated by research results that indicate the 1992 Flores earthquake resulted in a fault rupture that was inclined toward the ENE (east-northeast) [27, 40]. This finding is related to the 2018 Lombok earthquake phenomenon [31, 41]. Nevertheless, other results indicate that the Flores back-arc thrust fault has a greater impact on the region's earthquake potential [5, 42]. The 1992 Flores earthquake was a more destructive seismic event than Nicaragua, according to another study [8]. Furthermore, this phenomenon served as the catalyst for the establishment of the Tsunami Bulletin Board (TBB) network [2]. The reason for this is that the absence of contemporary equipment leads to a limited quantity of recorded data, as demonstrated by the existence of only one tidal gauge in Palopo, Sulawesi [5, 43].

2.3. Obstacles to Seismic Monitoring in the Flores Sea

The region's intensive tectonic and volcanic activities have resulted in a high level of seismic background noise, which is one of the primary challenges. The capacity of seismic stations to detect and analyze minor earthquakes, which are crucial in seismological research and disaster mitigation, can be impacted by this noise [44]. The primary cause of this seismic disturbance is the vibrations produced by volcanic activity and the movement of tectonic plates [45]. The data that is collected is frequently contaminated by seismic waves from non-earthquake geological activities, such as volcanic eruptions or earth surface movements, when monitoring stations are situated in close proximity to active zones like the Flores Trough or active volcanoes. Consequently, it is crucial to locate seismic stations in an appropriate location, outside the active zone, in order to reduce the disturbance. The Flores Sea's limited infrastructure is an additional obstacle to seismic monitoring, in addition to background noise. While efforts have been made to establish a network of seismic stations in the region, the majority of these stations are situated on land, which restricts their ability to detect earthquakes in remote areas or under the sea.

3. Methods

3.1. Research Area

The Flores Sea, located in eastern Indonesia, is renowned for its distinctive characteristics, which render it a significant region in terms of both ecology and geology. The Flores Sea is situated in the convergence of two significant tectonic plates, the Indo-Australian Plate and the Eurasian Plate, as part of the Pacific Ring of Fire [46, 47]. Active subduction zones, underwater volcanoes, and active faults are among the distinctive geological phenomena that result from the interaction of these two continents [48, 49]. The seismic data used in this study is data sourced from three stations that can capture seismic data in the Flores Sea region (Fig. **1**, Table **1**).

Table 1: Research seismic station data.

Station Code	Latitude	Longitude	Start Date	End Date
COCO	-12.1901	96.8349	1996-12-15	2599-12-31
KAPI	-5.0142	119.7517	1999-02-06	2599-12-31
WRAB	-19.9336	134.36	1994-03-27	2599-12-31

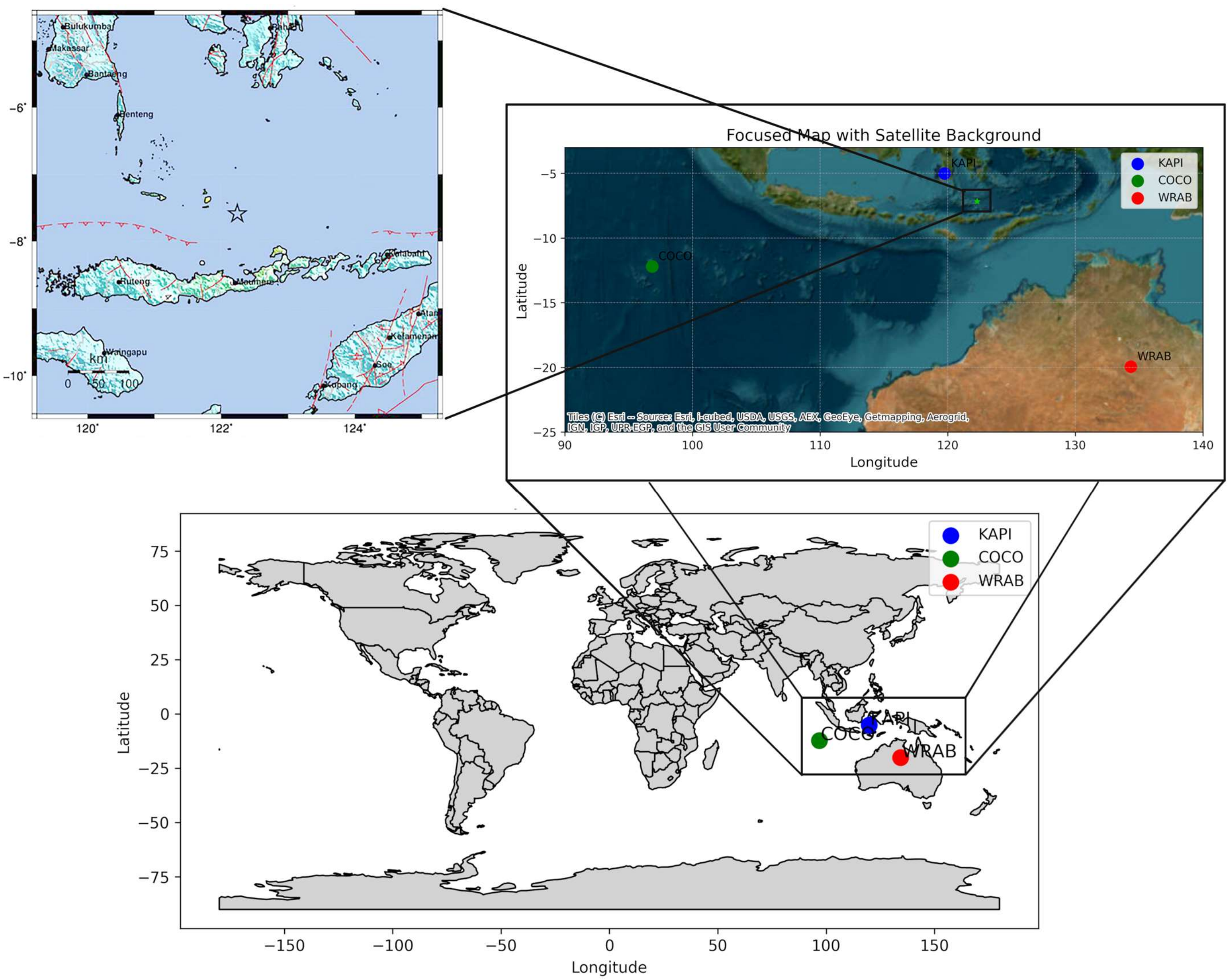

Figure 1: Map of the study area with the green star depicts the 14 December 2021 (Mw 7.3) epicenter and seismic station.

3.2. Sampling and Monitoring Methods

The seismic data from December 14-16, 2021, was accessed through the IRIS (Incorporated Research Institutions for Seismology) web service for this study. The IRIS Modular Utility for Statistical Knowledge Gathering (MUSTANG) system was employed during the analysis phase, as illustrated in Fig. (**2**). In general, tools that are devised based on the appropriate Power Spectral Densities (PSD) and Probability Density Functions (PDF) are used to evaluate background noise at seismic stations [24]. IRIS [50] has developed an open source software suite known as MUSTANG.

MUSTANG is intended to satisfy the requirements of long-term statistical analysis, with an emphasis on the monitoring of real-time and historical data integrity. The primary objective of MUSTANG is to assess and quantify the quality parameters of seismic data by employing a variety of metrics, including noise level, dynamic range, and timing accuracy [50, 51]. In order to guarantee that the data collected satisfies specific quality standards and can be utilized in scientific research without substantial bias or error, these parameters are examined. MUSTANG's capacity to detect anomalies in seismic data, including instrumental interference, environmental noise, or calibration inconsistencies, is one of its most remarkable capabilities. Therefore, MUSTANG contributes to the enhancement of confidence in the reliability of seismic data, which serves as the foundation for disaster mitigation and seismological research [52, 53]. To describe how the levels of seismic background noise change in the BH1 (north-south horizontal direction), BH2 (east-west horizontal direction), and BHZ (up-down vertical direction) directions [24, 50, 53]. The PDF analysis is crucial for the characterization of noise at each station. Additionally, the PDF can view the results of a statistical approach that calculates the probability density function to assess the full spectrum of noise at each station [54, 55].

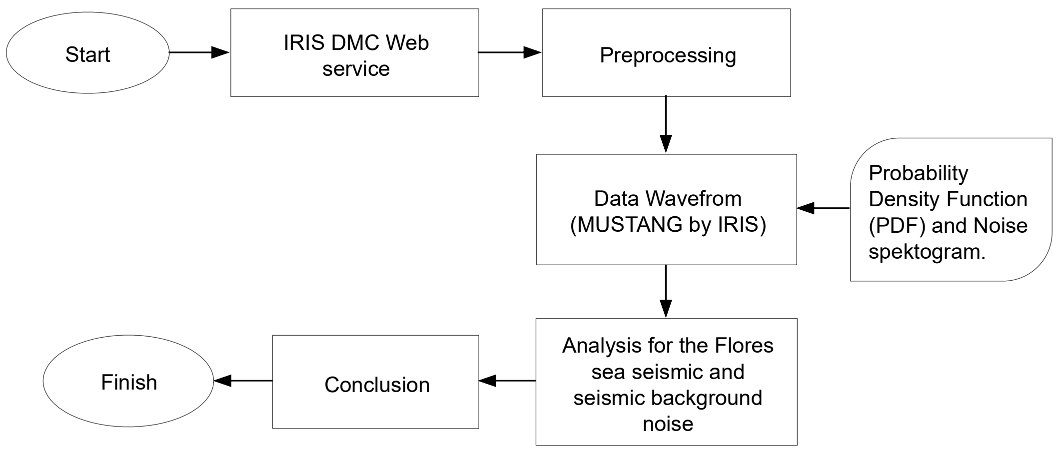

Figure 2: Research flow.

4. Results and Discussion

The level of earthquake activity that naturally and routinely occurs in a region or area over a long period of time is referred to as seismic background [56]. This encompasses small and medium-sized earthquakes that occur without any noteworthy significant earthquake activity or extraordinary earthquake events. The nearest monitoring station location records continuous vibrations or signals detected by seismometers, which may include earthquake activity and other noise [57, 58]. In order to determine the distribution of noise in the seismic data recording at each station, seismic background noise is analyzed using the data that has been collected [59].

The noise spectrogram, PSD, and PDF were employed to conduct the analysis in the BH1, BH2, and BHZ orientations. The direction component is the station code that is employed to identify the seismometer component and the direction of seismic wave recording. The research data consists of event data obtained from recording stations, including the COCO, KAPI, and WRAB stations in the IRIS client.

SNR is a metric that is employed to compare the strength of the intended earthquake signal with the noise level (interference) in seismic data [60]. The distribution of seismic data for SNR, as determined by P waves, indicates that the SNR increases as the magnitude of the earthquake increases [61]. Specifically, earthquakes with high magnitudes generate more robust signals [62, 63]. The earthquake signal can be more easily identified and distinguished from the noise level in the data as the SNR increases. Probability Density Functions (PDF), Power Spectral Density (PSD), and noise spectrogram data can be employed to determine the SNR at a monitoring station (Fig. **3**). The distribution of SNR values at a station can be analyzed using PDF to demonstrate the probability of the occurrence of various SNR values at the station. The PSD shows how the energy is spread out at different frequencies. A higher SNR means that the signal peaks are clearer than the noise at different frequency ranges. The frequency spectrum of noise or interference will be described by the noise spectrogram, which is based on the frequency composition [53, 64].

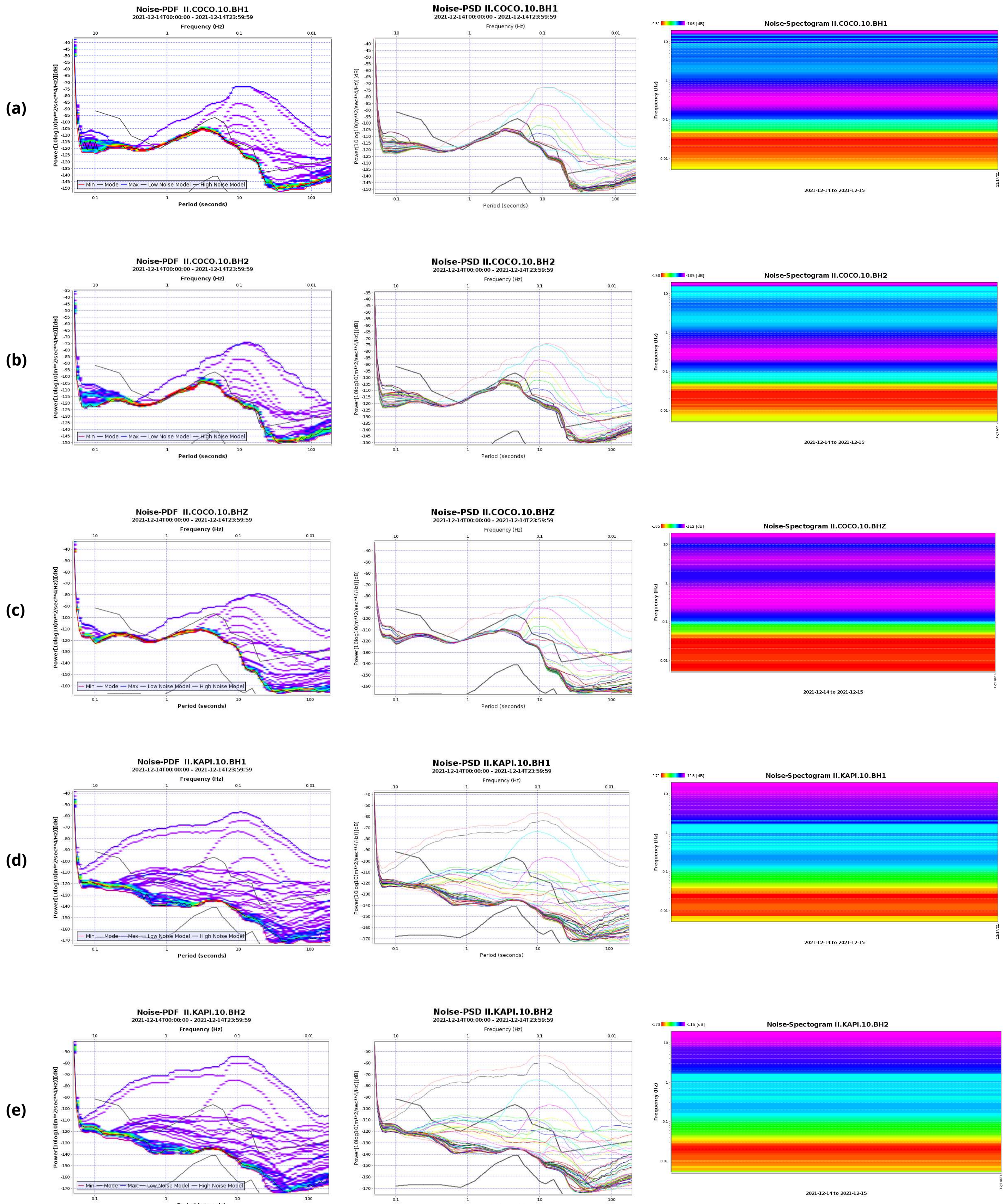
(a)
Noise-PDF II.COCO.10.BH1
2021-12-14T00:00:00 - 2021-12-14T23:59:59
Noise-PSD II.COCO.10.BH1
2021-12-14T00:00:00 - 2021-12-14T23:59:59
Noise-Spectogram II.COCO.10.BH1
2021-12-14 to 2021-12-15
(b)
Noise-PDF II.COCO.10.BH2
2021-12-14T00:00:00 - 2021-12-14T23:59:59
Noise-PSD II.COCO.10.BH2
2021-12-14T00:00:00 - 2021-12-14T23:59:59
Noise-Spectogram II.COCO.10.BH2
2021-12-14 to 2021-12-15
(c)
Noise-PDF II.COCO.10.BHZ
2021-12-14T00:00:00 - 2021-12-14T23:59:59
Noise-PSD II.COCO.10.BHZ
2021-12-14T00:00:00 - 2021-12-14T23:59:59
Noise-Spectogram II.COCO.10.BHZ
2021-12-14 to 2021-12-15
(d)
Noise-PDF II.KAPI.10.BH1
2021-12-14T00:00:00 - 2021-12-14T23:59:59
Noise-PSD II.KAPI.10.BH1
2021-12-14T00:00:00 - 2021-12-14T23:59:59
Noise-Spectogram II.KAPI.10.BH1
2021-12-14 to 2021-12-15
(e)
Noise-PDF II.KAPI.10.BH2
2021-12-14T00:00:00 - 2021-12-14T23:59:59
Noise-PSD II.KAPI.10.BH2
2021-12-14T00:00:00 - 2021-12-14T23:59:59
Noise-Spectogram II.KAPI.10.BH2
2021-12-14 to 2021-12-15
Frequency (Hz)
Period (seconds)
Power[10log10(m**2/sec**4/Hz)][dB]
Min — Mode — Max — Low Noise Model — High Noise Model

Figure 3 (contd….)

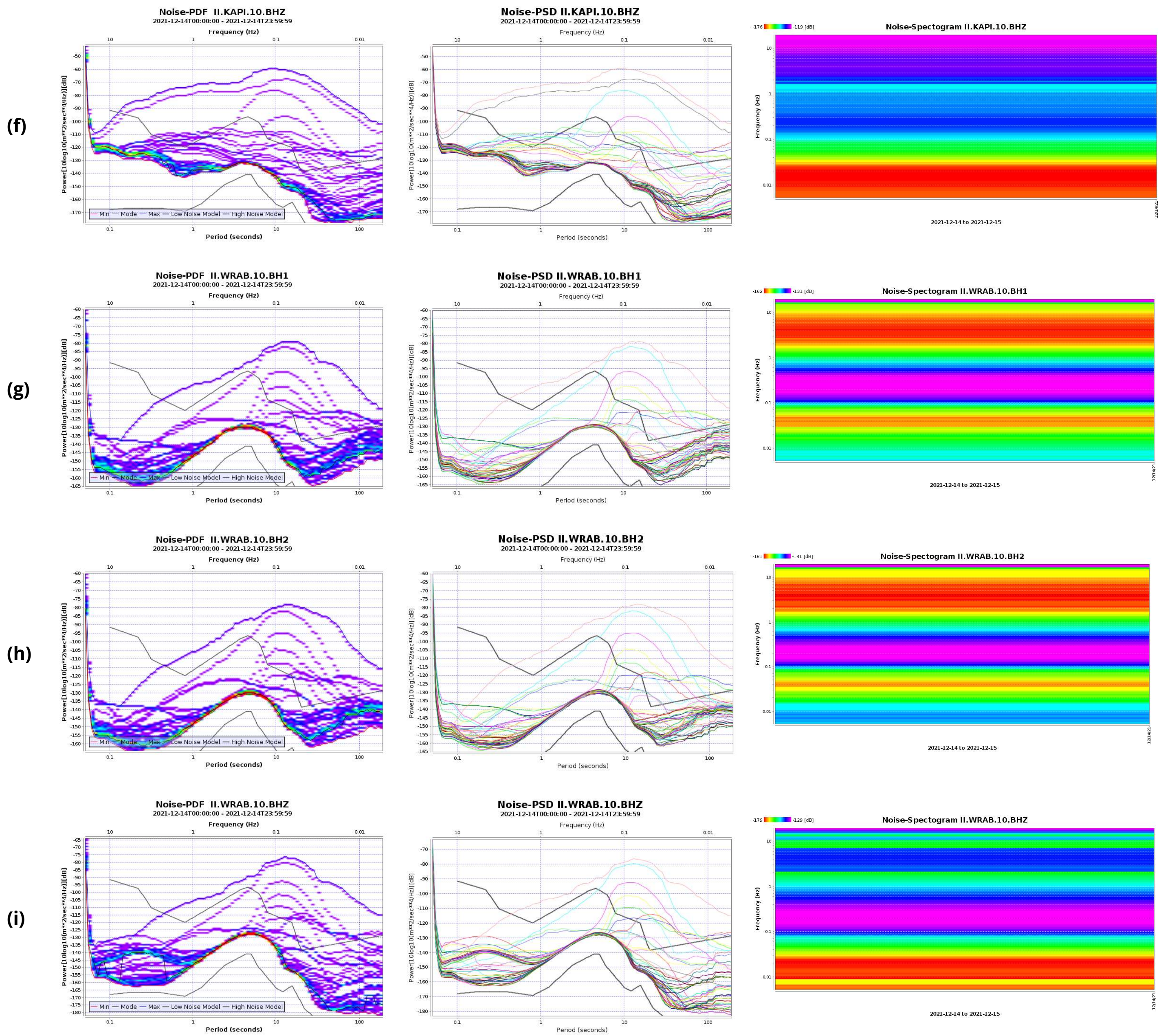

Figure 3: Probability Density Functions (PDF), Power Spectral Density (PSD), and Residual noise spectrogram on December 14-15, 2021 with (**a**) COCO stations in the direction of BH1, (**b**) COCO stations in the direction of BH2, (**c**) COCO stations in the direction BHZ, (**d**) KAPI station in BH1 direction, (**e**) KAPI station in BH2 direction, (**f**) KAPI station in BHZ direction, (**g**) WRAB station in BH1 direction, (**h**) WRAB station in BH2 direction, and (**i**) WRAB station in the BHZ direction.

The PDF, PSD, and noise spectrogram results obtained with MUSTANG are illustrated in Fig. (**3** and **4**). The purpose of this study is to examine the noise characteristics that are not influenced by time at the station. The results of the analysis, which were derived from the request for noise spectrum compilation data on earthquake events, are presented in this study. The seismic data recording for December 14-15, 2021, is depicted in Fig. (**3**). The data recording includes a significant main earthquake (Mw7.3), while Fig. (**4**) depicts a seismic data recording for December 15-16, 2021, with a magnitude value of approximately ≤4. Results in the form of noise spectrograms demonstrate that the time series contains a substantial quantity of information [65]. The PSD distribution in the seismic channel is characterized using PDF analysis [66]. The frequency and intensity of noise waves that surround the monitoring station are referred to as the spectral characteristics of noise [67]. The polarization of Rayleigh waves is depicted in Fig. (**3** and **4**), which demonstrate the variation in noise levels based on the direction of the BH1, BH2, and BHZ components [54].

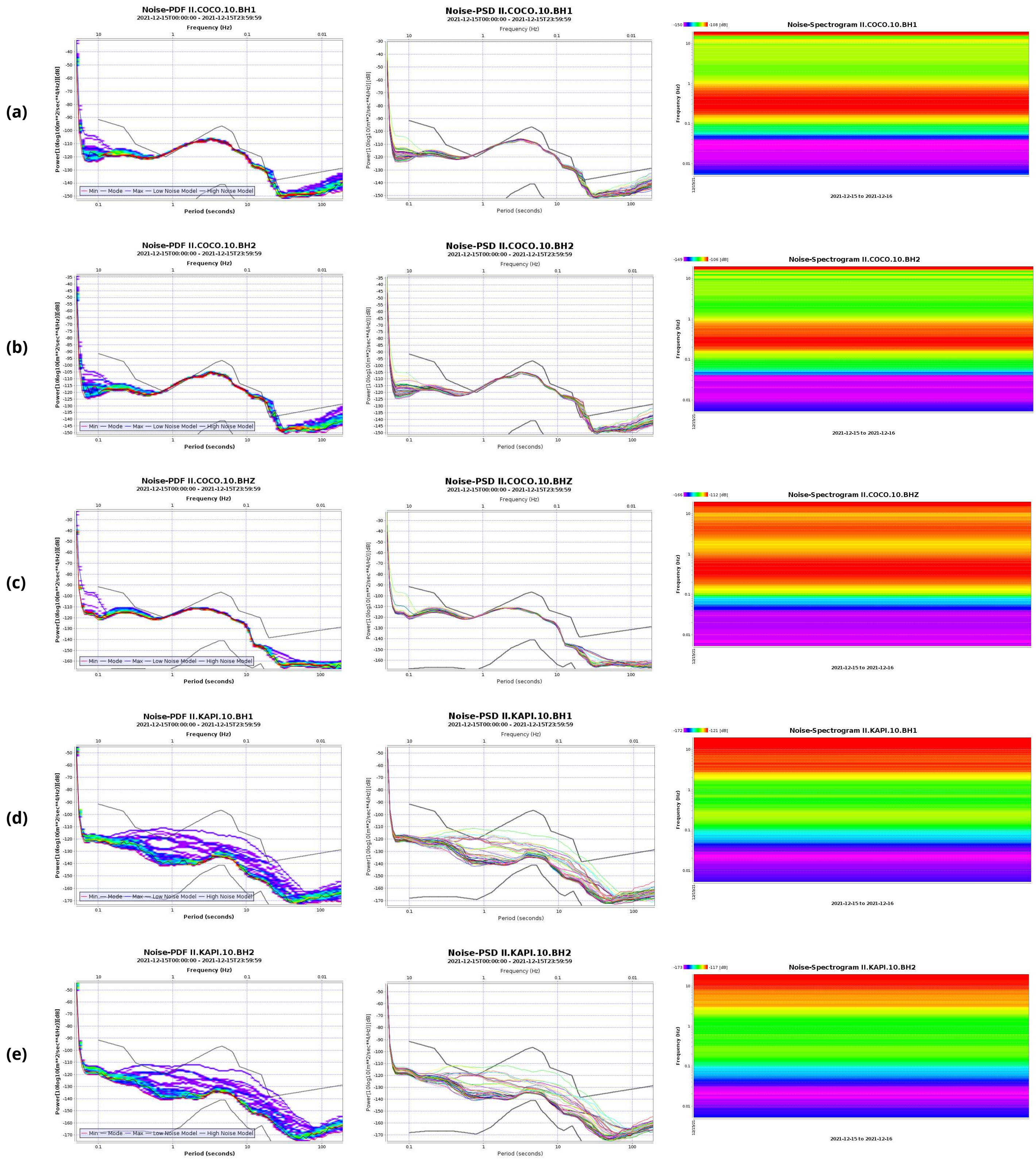

Figure 4 (contd….)

(f)

(g)

(h)

(i)

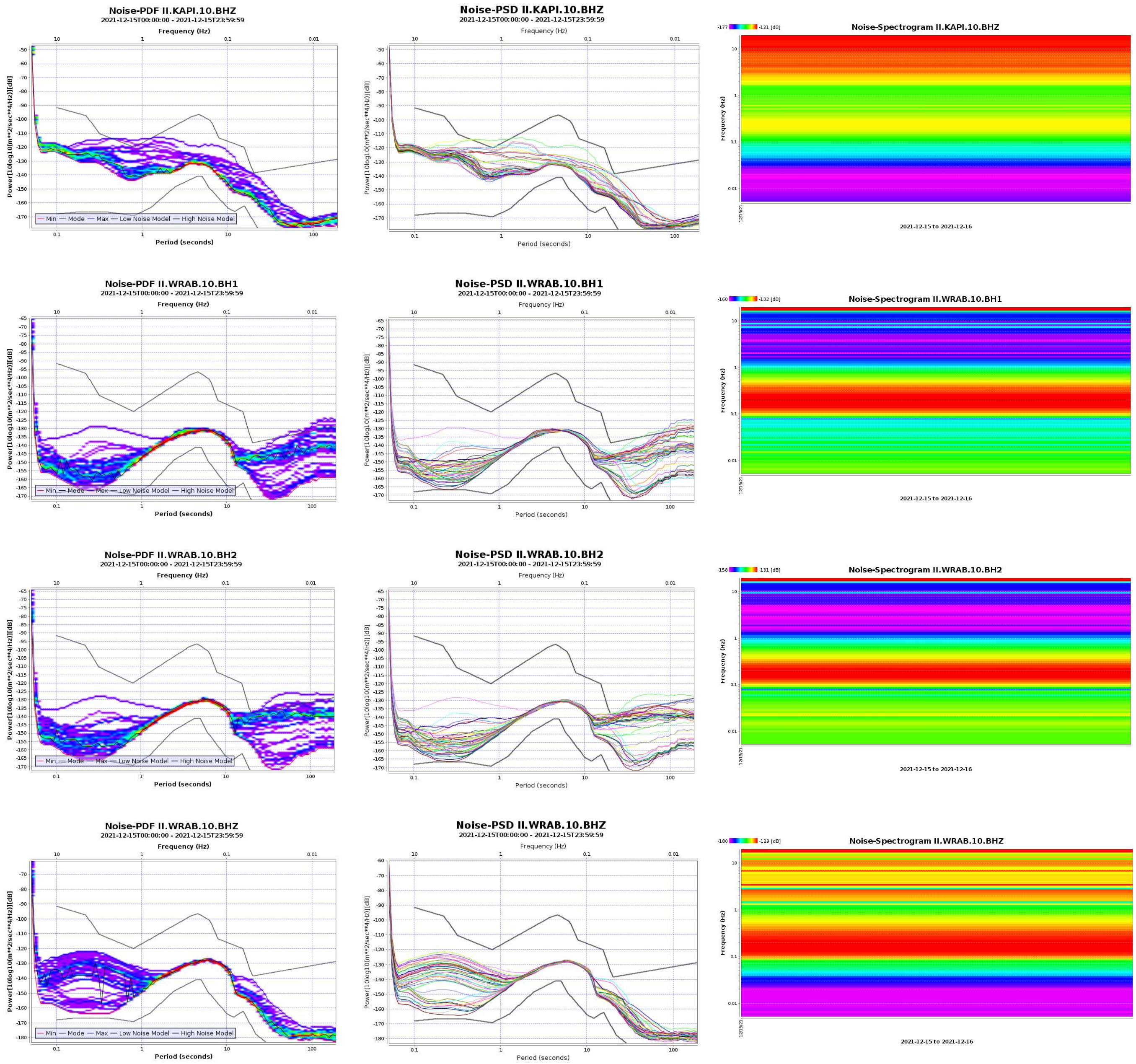

Figure 4: Probability Density Functions (PDF), Power Spectral Density (PSD), and Residual noise spectrogram on December 15-16, 2021 with (**a**) COCO stations in the direction of BH1, (**b**) COCO stations in the direction of BH2, (**c**) COCO stations in the direction BHZ, (**d**) KAPI station in BH1 direction, (**e**) KAPI station in BH2 direction, (**f**) KAPI station in BHZ direction, (**g**) WRAB station in BH1 direction, (**h**) WRAB station in BH2 direction, and (**i**) WRAB station in the BHZ direction.

Long period (0.01-0.1 Hz), microseismic (0.1-1.0 Hz), and short period (1.0-10 Hz) are the three frequency categories into which the noise spectrum is typically divided. There are six different period bands that can be found. These are the short period (0.1-1 s), the body wave dominant period (1-5 s), the secondary and primary microseismic (5-10 s and 10-20 s), the medium period (20-50 s), and the long period (50-100 s) [53, 68]. In all three components, each station exhibits minimal noise levels within the 1 to 10 s range (Fig. **3** and **4**) [69]. The vertical channel exhibits minimal noise levels during the protracted period of 10 to 100 s, whereas the horizontal component is more akin to the high noise model. The noise observed in the brief period (0.1-1 s) is influenced by wind and noise generated from cultural activities [67]. The results indicate that each station produces fluctuations at frequencies below 1 Hz in addition to those above 2 Hz. The results demonstrate the impact of external factors, such as wind or cultural activities, on short-period noise levels, as well as the variation of noise between horizontal and vertical components over a specific period.

The noise spectrum across various frequency bands is of considerable significance, as it provides a thorough understanding of the dynamics within the seismic station environment and the reliability of the resulting data. The exhaustive examination of the noise sources and attributes is facilitated by the categorization of noise into six period bands, which range from short period (0.1–1 s) to long period (50–100 s). The station is capable of capturing high-quality body wave signals, as evidenced by the low noise levels in all components during the 1–10 s time interval. On the other hand, the horizontal component has more noise during long periods of time (10–100 s), which suggests that it is more vulnerable to tectonic activity or topographic changes. Important indicators for optimizing station placement include noise variations at high (>2 Hz) and low (<1 Hz) frequencies, as well as the influence of external factors such as wind and cultural activities over brief periods.

The location and implementation of the seismic station have a significant impact on the noise level [70, 71]. Nevertheless, the signal is also plagued by issues such as interference, mass concentration, and damaged components that develop over time [72]. The instrument response information used to convert the recorded quantities may also be inaccurate. The PDF estimated from the PSD of ambient noise at a location can be used to evaluate all vibrations caused by natural sources (e.g., earthquakes) or artificial disturbances [73, 74]. Some noise sources may be unavoidable due to their origin, while others can be managed by relocating the afflicted station [75]. The PSD is calculated to obtain statistical information about frequency by utilizing the PDF in seismic noise monitoring. Nevertheless, the PDF is less suitable for monitoring small changes due to the substantial variation in noise level over time and with frequency [76].

In-depth insights into the performance of COCO, KAPI, and WRAB stations on 15–16 December 2021 are provided by noise intensity analysis using PDF, PSD, and residual noise spectrograms. The BH1 and BH2 directions (horizontal components) at COCO station exhibit substantial noise variations, which are indicative of sensitivity to surface activities such as wind or artificial disturbances. Conversely, the BHZ direction (vertical component) exhibits more stable noise, which is consistent with the low-noise model at longer frequencies (>10 seconds). The analysis at the KAPI station shows a pattern that is similar to that of COCO. The horizontal components (BH1 and BH2) are more likely to be affected by transient noise than the vertical components (BHZ). This pattern may be explained by the potential damage to sensor components or the influence of station location. The PSD at KAPI suggests that there are substantial noise fluctuations at high frequencies (>1 Hz), which may be attributed to local environmental factors. The optimal quality of the station location is evident in the reduced noise levels observed in all directions (BH1, BH2, BHZ) at the WRAB station. Nevertheless, the horizontal component remains in close proximity to the high-noise model at specific frequencies, suggesting interference from external sources. The significance of assessing PDF and PSD to comprehend the noise distribution in a specific direction and frequency is underscored by the comparison of these three stations. The residual noise spectrogram enables the identification of temporal fluctuations [57], which is beneficial in the identification of environmental factors that impact data quality.

The mathematical foundation for comprehending the propagation of elastic waves in the Earth is the seismic wave equation, which is essential for modeling subsurface dynamics in the Flores Sea. The accuracy of earthquake and tsunami predictions can be enhanced through model adjustments based on noise intensity data from stations such as COCO, KAPI, and WRAB. Body waves (P and S) and surface waves (Rayleigh and Love) are essential for obtaining information about geological structures, including subduction zones, active faults, and crustal strata [77, 78]. These equations are employed to map the complexity of the tectonic system and to identify regions that are at high risk of earthquakes and tsunamis. Their practical implementations are particularly pertinent, particularly in the context of disaster mitigation. Rapid P-wave analysis can expedite the development of early warning systems [79], thereby allowing coastal populations to evacuate in a timely manner. Furthermore, S-wave velocities are crucial for the evaluation of soil characteristics and geological stability, which is essential for the planning of infrastructure in vulnerable regions.

The noise analysis results at the COCO, KAPI, and WRAB stations are congruent with the findings of Hakim *et al*. [80] in their Flores seismic noise study. They indicate that stations with low noise within model constraints can be utilized to analyze minor to medium earthquakes (magnitudes 3-5). Noise at low frequencies (<1 Hz) is often linked to tectonic activity, while noise at high frequencies (>2 Hz) is more affected by ambient factors including human activity and meteorological conditions. Despite the fact that the majority of stations recorded signal spectra between low and high noise models, cultural activities, particularly during brief intervals (about 1 second).

The findings are interpreted within a geological and tectonic context, revealing a close relationship between seismic activity and noise patterns in the Flores Sea region. This active subduction zone contains the Flores Back Arc Thrust fault, which is the principal source of seismic instability. It is also influenced by the contact of the Indo-Australian Plate and the Eurasian Plate [13]. The sensitivity of noise to external influences seen at COCO and KAPI stations corresponds to the impact of station location on data quality [80]. These findings highlight the importance of seismic monitoring in the Flores Sea region for disaster risk mitigation within the context of geotechnical zoning. The optimization of station sites, such as WRAB, can improve geotechnical risk mapping in this region by recording low noise in all components across short to long time periods. The combination of noise data, S-wave velocity, and regional geological and tectonic settings will provide a more solid foundation for infrastructure development and risk reduction in vulnerable places like the Flores Sea.

5. Conclusion

Normal faults dominate the Flores Sea region, which is a component of an active tectonic plate confluence zone. These faults generate seismic activity of varying magnitudes. These events are recorded by seismic stations such as KAPI, COCO, and WRAB, as demonstrated by the MUSTANG analysis, with a relatively high signal-to-noise ratio (SNR). Despite this, the study found that high background noise, which includes things like human activities, natural oceanic noises, and industrial operations that aren't related to earthquakes, is a huge problem. The frequency and intensity of noise that dominates the station locations are revealed by spectral noise analysis. This obscures the seismic signals and necessitates more intricate analysis methods, such as advanced signal processing techniques or machine learning applications, to differentiate seismic signals from noise. Direct implications for earthquake risk mitigation are demonstrated by this investigation. The results can be employed to optimize the placement of seismic stations to reduce noise interference, thereby enhancing the precision of earthquake and tsunami early warning systems. Furthermore, the data produced can be used to aid policymakers in the creation of evidence-based mitigation strategies, including the development of more precise seismic risk maps and effective emergency evacuation plans. Therefore, this research plays a role in the enhancement of disaster preparedness infrastructure that is scientifically founded.

Conflicts of Interest

The authors declare that they have no known competing financial interests or personal relationships that could have appeared to influence the work reported in this paper.

Funding

This project received no funding.

Acknowledgments

The researcher would like to express gratitude to the IRIS Data Services Facility, and in particular the IRIS Data Management Center.

Author’s Contribution

AK: Resources, Software, Conceptualization, Project administration, Methodology, funding acquisition, Writing - original draft, Review & editing.

AJ: Conceptualization, Methodology, Software, Data curation.

AA and OWJT: Conceptualization, Methodology, Software, Review & editing.

KWW: Conceptualization, Methodology, Review & editing.

References

[1] Kim KO, Kim DC, Yuk JH, Pelinovsky E, Choi BH. Extreme tsunami inundation at babi island due to flores earthquake induced tsunami in 1992. Ocean Polar Res. 2015; 37(2): 91-105. https://doi.org/10.4217/OPR.2015.37.2.091

[2] Okal EA. Twenty-five years of progress in the science of "geological" tsunamis following the 1992 nicaragua and flores events. Pure Appl Geophys. 2019; 176(7): 2771-93. https://doi.org/10.1007/s00024-019-02244-x

[3] Kânoğlu U, Tanioka Y, Okal EA, Baptista MA, Rabinovich AB. Introduction to "twenty five years of modern tsunami science following the 1992 nicaragua and flores island tsunamis, volume i." Pure Appl Geophys. 2019; 176(7): 2757-69. https://doi.org/10.1007/s00024-019-02266-5

[4] Kânoğlu U, Tanioka Y, Okal EA, Baptista MA, Rabinovich AB. Introduction to "twenty five years of modern tsunami science following the 1992 nicaragua and flores island tsunamis, volume ii." Pure Appl Geophys. 2020; 177(3): 1183-91. https://doi.org/10.1007/s00024-020-02451-x

[5] Pranantyo IR, Cummins PR. Multi-data-type source estimation for the 1992 flores earthquake and tsunami. Pure Appl Geophys. 2019; 176(7): 2969-83. https://doi.org/10.1007/s00024-018-2078-4

[6] Julius AM, Daryono. Overview of 1990s deadly tsunamis in Indonesia. In: E3S Web of Conferences. 2021. p. 07001. https://doi.org/10.1051/e3sconf/202133107001

[7] Minoura K, Imamura F, Takahashi T, Shuto N. Sequence of sedimentation processes caused by the 1992 flores tsunami: evidence from babi island. Geology. 1997; 25(6): 523-6. https://doi.org/10.1130/0091-7613(1997)025<0523:SOSPCB>2.3.CO;2

[8] Satake K, Bourgeois J, Abe K, Abe K, Tsuji Y, Imamura F, *et al*. Tsunami field survey of the 1992 Nicaragua earthquake. Eos, Transactions American Geophysical Union. 1993; 74(13): 145-57. https://doi.org/10.1029/93EO00271

[9] Handayani L. Seismic Hazard Analysis of Maumere, Flores: a Review of the Earthquake Sources. In: Proceedings of the Proceedings of the 7th Mathematics, Science, and Computer Science Education International Seminar, MSCEIS 2019, 12 October 2019, Bandung, West Java, Indonesia: EAI; 2020. https://doi.org/10.4108/eai.12-10-2019.2296247

[10] Bassal P, Papageorgiou E, Moug DM, Bray JD, Cetin KO, Şahin A, *et al*. Liquefaction ground deformations and cascading coastal flood hazard in the 2023 Kahramanmaraş earthquake sequence. Earthquake Spectra. 2024; 40(3): 1845-69. https://doi.org/10.1177/87552930241247830

[11] Maneno R, Sentosa BJ, Rachman G. Relocation of earthquake hypocenter in the flores region using hypo71. IPTEK J Eng. 2019; 5(2): 33-7. https://doi.org/10.12962/joe.v5i2.5024

[12] Jufriansah A, Khusnani A, Pramudya Y, Afriyanto M, History A, Jufriansah A, *et al*. Estimation of flores sea aftershock rupture data based on AI. Indones Rev Phys. 2023; 6(1): 46-56. https://doi.org/10.12928/irip.v6i1.6705

[13] Supendi P, Rawlinson N, Prayitno BS, Widiyantoro S, Simanjuntak A, Palgunadi KH, *et al*. The kalaotoa fault: a newly identified fault that generated the mw 7.3 flores sea earthquake. The Seismic Record. 2022; 2(3): 176-85. https://doi.org/10.1785/0320220015

[14] Jufriansah A, Khusnani A, Pramudya Y, Afriyanto M. Comparison of aftershock behavior of the flores sea 12 december 1992 and 14 december 2021. J Phys. 2023; 7(1): 65-74. https://doi.org/10.20961/jphystheor-appl.v7i1.71609

[15] Khusnani A, Jufriansah A, Afriyanto M. Utilization of seismic data as a tsunami vulnerability review. Indones Rev Phys. 2022; 5(2): 66-72. https://doi.org/10.12928/irip.v5i2.6706

[16] Maulana BR, Burhanuddin MS, Akbar MuhF. Lineament density and implications for the distribution of ground fissures after 2021 MW 7.3 flores sea earthquake on Kalaotoa Island, Indonesia. J Geosci Eng Environ Technol. 2023; 8(1): 17-26. https://doi.org/10.25299/jgeet.2023.8.1.10849

[17] Chen Y, Liu M, Wang H. Aftershocks and background seismicity in tangshan and the rest of North China. J Geophys Res Solid Earth. 2021;126(5): 1-15. https://doi.org/10.1029/2020JB021395

[18] Liu Y, Zhuang J, Jiang C. Background seismicity before and after the 1976 ms 7.8 tangshan earthquake: is its aftershock sequence still continuing? Seismol Res Lett. 2021; 92(2A): 877-85. https://doi.org/10.1785/0220200179

[19] Ringler AT, Steim J, Wilson DC, Widmer-Schnidrig R, Anthony RE. Improvements in seismic resolution and current limitations in the Global Seismographic Network. Geophys J Int. 2020; 220(1): 508-21. https://doi.org/10.1093/gji/ggz473

[20] Diaz J, Ruiz M, Udina M, Polls F, Martí D, Bech J. Monitoring storm evolution using a high-density seismic network. Sci Rep. 2023; 13(1): 1853. https://doi.org/10.1038/s41598-023-28902-8

[21] Ichihara M, Ohminato T, Konstantinou KI, Yamakawa K, Watanabe A, Takeo M. Seismic background level (SBL) growth can reveal slowly developing long-term eruption precursors. Sci Rep. 2023; 13(1): 5954. https://doi.org/10.1038/s41598-023-32875-z

[22] Rowse SL, Heath R. Has the importance of 'signal' been forgotten in the signal-to-noise ratio of land seismic acquisition? First Break. 2024; 42(1): 79-84. https://doi.org/10.3997/1365-2397.fb2024007

[23] Wang H, Zhang J. A deep learning approach for suppressing noise in livestream earthquake data from a large seismic network. Geophys J Int. 2023; 233(3): 1546-59. https://doi.org/10.1093/gji/ggad009

[24] McNamara DE, Buland RP. Ambient noise levels in the continental United States. Bull Seismol Soc Am. 2004; 94(4): 1517-27. https://doi.org/10.1785/012003001

[25] Yao Q, Wang Y, Yang Y, Shi Y. Seal call recognition based on general regression neural network using Mel-frequency cepstrum coefficient features. EURASIP J Adv Signal Process. 2023; 2023(1): 48. https://doi.org/10.1186/s13634-023-01014-1

[26] Agarwal D, Suresh J, Mitra S, Ain A. Angular power spectra of anisotropic stochastic gravitational wave background: Developing statistical methods and analyzing data from ground-based detectors. Phys Rev D. 2023; 108(2): 023011. https://doi.org/10.1103/PhysRevD.108.023011

[27] Beckers J, Lay T. Very broadband seismic analysis of the 1992 Flores, Indonesia, earthquake (Mw = 7.9). J Geophys Res Solid Earth. 1995; 100(B9): 18179-93. https://doi.org/10.1029/95JB01689

[28] Jufriansah A, Khusnani A, Saputra S, Suwandi Wahab D. Forecasting the magnitude category based on the flores sea earthquake. J RESTI. 2023; 7(6): 1439-47. https://doi.org/10.29207/resti.v7i6.5495

[29] Saputra R, Lubis MHM, Wulan EP. Early result of imaging 3D seismic velocity structure in central java using double-difference tomography. IOP Conf Ser Earth Environ Sci. 2023; 1227(1): 012039. https://doi.org/10.1088/1755-1315/429/1/012039

[30] Wulan EP, Madrinovella I, Saputra R, Asyidah SN, Haqi YS, Wijaya FC, *et al*. The early model of tomography in eastern indonesia using FMTOMO. IOP Conf Ser Earth Environ Sci. 2023; 1227(1): 012037. https://doi.org/10.1088/1755-1315/1227/1/012037

[31] Felix RP, Hubbard JA, Bradley KE, Lythgoe KH, Li L, Switzer AD. Tsunami hazard in Lombok and Bali, Indonesia, due to the Flores back-arc thrust. Nat Hazards Earth Sys Sci. 2022; 22(5): 1665-82. https://doi.org/10.5194/nhess-22-1665-2022

[32] Rebetsky YuL, Stefanov YuP. On the mechanism of interaction between strong earthquakes and volcanism in subduction zones. Russ J Pac Geol. 2023; 17(S2): S107-21. https://doi.org/10.1134/S1819714023080109

[33] Afif H, Nugraha AD, Muzli M, Widiyantoro S, Zulfakriza Z, Wei S, *et al*. Local earthquake tomography of the source region of the 2018 Lombok earthquake sequence, Indonesia. Geophys J Int. 2021; 226(3): 1814-23. https://doi.org/10.1093/gji/ggab189

[34] Andikagumi H, Bradley K. The flores thrust and its interplay with volcanism. Tectonics. 2024; 43(11): 1-18. https://doi.org/10.1029/2024TC008269

[35] Jufriansah A, Anggraini A, Zulfakriza Z, Khusnani A, Pramudya Y. Forecast earthquake precursor in the Flores Sea. Indones J Electr Eng Comput Sci. 2023; 32(3): 1825. https://doi.org/10.11591/ijeecs.v32.i3.pp1825-1836

[36] Wibowo M. Modeling the potential of tsunami hazard in labuan bajo towards a disaster-resilient tourism area. Indones J Geogr. 2022; 54(1): 83-91. https://doi.org/10.22146/ijg.71220

[37] Wulan EP, Madrinovella I, Saputra R, Asyidah SN, Haqi YS, Wijaya FC, *et al*. The early model of tomography in Eastern Indonesia using FMTOMO. IOP Conf Ser Earth Environ Sci. 2023; 1227(1): 012037. https://doi.org/10.1088/1755-1315/1227/1/012037

[38] Hutchings SJ, Mooney WD. The Seismicity of Indonesia and Tectonic Implications. Geochem Geophys Geosys. 2021; 22(9): 1-42. https://doi.org/10.1029/2021GC009812

[39] Pranantyo IR, Cummins PR. The 1674 ambon tsunami: extreme run-up caused by an earthquake-triggered landslide. Pure Appl Geophys. 2020; 177(3): 1639-57. https://doi.org/10.1007/s00024-019-02390-2

[40] Koulali A, Susilo S, McClusky S, Meilano I, Cummins P, Tregoning P, *et al*. Crustal Strain Partitioning and the Associated Earthquake Hazard in the Eastern Sunda-Banda Arc. Geophys Res Lett. 2016; 43(5):1943-9. https://doi.org/10.1002/2016GL067941

[41] Yang X, Singh SC, Tripathi A. Did the flores backarc thrust rupture offshore during the 2018 lombok earthquake sequence in Indonesia? Geophys J Int. 2020; 221(2): 758-68. https://doi.org/10.1093/gji/ggaa018

[42] Supendi P, Nugraha AD, Widiyantoro S, Abdullah CI, Rawlinson N, Cummins PR, *et al*. Fate of forearc lithosphere at arc-continent collision zones: evidence from local earthquake tomography of the sunda-banda arc transition, Indonesia. Geophys Res Lett. 2020; 47(6): 1-9. https://doi.org/10.1029/2019GL086472

[43] Pranantyo IR, Cummins P, Griffin J, Davies G, Latief H. Modelling of historical tsunami in Eastern Indonesia: 1674 Ambon and 1992 Flores case studies. AIP Conf Proc. 1857; 090005. https://doi.org/10.1063/1.4987104

[44] Saygin E, Cummins PR, Lumley D. Retrieval of the P wave reflectivity response from autocorrelation of seismic noise: Jakarta Basin, Indonesia. Geophys Res Lett. 2017; 44(2): 792-9. https://doi.org/10.1002/2016GL071363

[45] Johnson CW, Ben-Zion Y, Meng H, Vernon F. Identifying different classes of seismic noise signals using unsupervised learning. Geophys Res Lett. 2020; 47(15): 1-10. https://doi.org/10.1029/2020GL088353

[46] Riyan Eko Prasetiyo, Gita Amperiawan, Ansori A. Mapping of tsunami risk zones on lombok island to support military operations other than war (OMSP). Int J Educ Hum Soc Sci. 2024; 3(5): 2458-2472. https://doi.org/10.55227/ijhess.v3i5.975

[47] Fuady M, Munadi R, Fuady MAK. Disaster mitigation in Indonesia: between plans and reality. IOP Conf Ser Mater Sci Eng. 2021; 1087(1): 012011. https://doi.org/10.1088/1757-899X/1087/1/012011

[48] Lemenkova P. Deep-sea trenches of the pacific ocean: a comparative analysis of the submarine geomorphology using data modeling by Gmt, Python and R (thesis). SSRN Electronic Journal; June 2, 2021. https://doi.org/10.2139/ssrn.3858289

[49] Xia Y, Kopp H, Klaeschen D, Geersen J, Ma B, Schnabel M. Seamount and ridge subduction at the Java Margin, Indonesia: Effects on structural geology and seismogenesis. J Geophys Res Solid Earth. 2023; 128(9): 1-23. https://doi.org/10.1029/2022JB026272

[50] Wolin E, McNamara DE. Establishing high-frequency noise baselines to 100 Hz based on millions of power spectra from IRIS MUSTANG. Bull Seismol Soc Am. 2020; 110(1): 270-8. https://doi.org/10.1785/0120190123

[51] Casale P, Pignatelli A. Use of deep learning to improve seismic data quality analysis. Ann Geophys. 2024; 67(3): SE320. https://doi.org/10.4401/ag-9055

[52] Anthony RE, Ringler AT, Wilson DC, Bahavar M, Koper KD. How processing methodologies can distort and bias power spectral density estimates of seismic background noise. Seismol Res Lett. 2020; 91(3): 1694-706. https://doi.org/10.1785/0220190212

[53] Tolea A, Grecu B, Neagoe C, Moldovan IA, Toader VE. Seismic noise analysis in the microseismic and high- frequency domain at the burar seismic stations. Rom Rep Phys. 2023; 75: Article no. 705. https://doi.org/10.59277/RomRepPhys.2023.75.705

[54] Casey R, Templeton ME, Sharer G, Keyson L, Weertman BR, Ahern T. Assuring the quality of IRIS Data with MUSTANG. Seismol Res Lett. 2018; 89(2A): 630-9. https://doi.org/10.1785/0220170191

[55] Sharer G, Templeton M, Keyson L, Carter J. Data quality assurance at the IRIS DMC: Expanding and improving the MUSTANG system. Authorea Preprints. 2022. https://doi.org/10.1002/essoar.10501324.1

[56] Supendi P, Nugraha AD, Widiyantoro S, Pesicek JD, Thurber CH, Abdullah CI, *et al*. Relocated aftershocks and background seismicity in eastern Indonesia shed light on the 2018 Lombok and Palu earthquake sequences. Geophys J Int. 2020; 221(3): 1845-55. https://doi.org/10.1093/gji/ggaa118

[57] Roy A, Sarkar S, Goap A, Ghosh R, Gaurav A, Akula A, *et al*. Seismic Instrumentation and Its Application. In: Handbook of Vibroacoustics, Noise and Harshness. Singapore: Springer; 2024. p. 1-36. https://doi.org/10.1007/978-981-99-4638-9_45-1

[58] Li Z. Recent advances in earthquake monitoring I: Ongoing revolution of seismic instrumentation. Earthq Sci. 2021; 34(2): 177-88. https://doi.org/10.29382/eqs-2021-0011

[59] Xu W, Davis P, Auerbach D, Klimczak E. Revision of metadata sensitivities at IRIS/IDA stations. Seismol Res Lett. 2018; 89(3):1084-92. https://doi.org/10.1785/0220170280

[60] Bilich A, Larson KM. Scientific utility of the signal-to-noise ratio (SNR) reported by geodetic GPS receivers GNSS interferometric reflectometry view project. 2007. Available from: https://www.researchgate.net/publication/265993074

[61] Panebianco S, Serlenga V, Satriano C, Cavalcante F, Stabile TA. Semi-automated template matching and machine-learning based analysis of the August 2020 Castelsaraceno microearthquake sequence (southern Italy). Geomat Nat Hazards Risk. 2023; 14(1): 2207715. https://doi.org/10.1080/19475705.2023.2207715

[62] Neupane AS. Crustal structure beneath the eastern nepal himalayas and southern tibet from receiver function analysis. Open Access Theses & Dissertations. 2015; pp.1-60. Available from: https://scholarworks.utep.edu/open_etd/1112

[63] Paul H, Priestley K, Powali D, Sharma S, Mitra S, Wanchoo S. Signatures of the existence of frontal and lateral ramp structures near the kishtwar window of the Jammu and Kashmir Himalaya: Evidence From Microseismicity and Source Mechanisms. Geochem Geophys Geosys. 2018; 19(9): 3097-114. https://doi.org/10.1029/2018GC007597

[64] Smith K, Tape C. Seismic noise in Central Alaska and influences from rivers, wind, and sedimentary basins. J Geophys Res Solid Earth. 2019; 124(11): 11678-704. https://doi.org/10.1029/2019JB017695

[65] Tsai VC, McNamara DE. Quantifying the influence of sea ice on ocean microseism using observations from the Bering Sea, Alaska. Geophys Res Lett. 2011; 38(22): L22502. https://doi.org/10.1029/2011GL049791

[66] Hutko AR, Bahavar M, Trabant C, Weekly RT, Fossen M Van, Ahern T. Data products at the IRIS‐DMC: growth and usage. Seismol Res Lett. 2017; 88(3): 892-903. https://doi.org/10.1785/0220160190

[67] McNamara DE. Ambient noise levels in the continental United States. Bull Seismol Soc Am. 2004; 94(4): 1517-27. https://doi.org/10.1785/0120200030

[68] Uthaman M, Singh C, Singh A, Jana N, Dubey AK, Sarkar S, *et al*. Spatial and temporal variation of the ambient noise environment of the Sikkim Himalaya. Sci Rep. 2022; 12(1): 1-13. https://doi.org/10.1038/s41598-021-04183-x

[69] Meltzer A, Stachnik JC, Sodnomsambuu D, Munkhuu U, Tsagaan B, Dashdondog M, *et al*. The central mongolia seismic experiment: multiple applications of temporary broadband seismic arrays. Seismol Res Lett. 2019; 90(3): 1364-76. https://doi.org/10.1785/0220180360

[70] Dimitrova L. Seismic noise at bulgarian antarctic seismic station and influence from site selection. In 2020. p. 623-30. https://doi.org/10.5593/sgem2020/1.2/s05.079

[71] Castellaro S, Alessandrini G, Musinu G. Seismic station installations and their impact on the recorded signals and derived quantities. Seismol Res Lett. 2022; 93(6): 3348-62. https://doi.org/10.1785/0220220029

[72] Czarny R, Malinowski M, Chamarczuk M, Ćwiękała M, Olechowski S, Isakow Z, *et al*. Dispersive seismic waves in a coal seam around the roadway in the presence of excavation damaged zone. Int J Rock Mech Min Sci. 2021; 148: 104937. https://doi.org/10.1016/j.ijrmms.2021.104937

[73] Koymans MR, Domingo Ballesta J, Ruigrok E, Sleeman R, Trani L, Evers LG. Performance assessment of geophysical instrumentation through the automated analysis of power spectral density estimates. Earth Space Sci. 2021; 8(9): 1-25. https://doi.org/10.1029/2021EA001675

[74] Łacny Ł, Ścisło Ł, Guinchard M. Application of probabilistic power spectral density technique to monitoring the long-term vibrational behaviour of cern seismic network stations. Vib Phys Sys. 2020; 31(3): 1-7.

[75] Abdel Hafiez HE, Toni M. Ambient noise level and site characterization in Northern Egypt. Pure Appl Geophys. 2019; 176(6): 2349-66. https://doi.org/10.1007/s00024-019-02112-8

[76] Pedersen HA, Leroy N, Zigone D, Vallée M, Ringler AT, Wilson DC. Using component ratios to detect metadata and instrument problems of seismic stations: examples from 18 Yr of GEOSCOPE data. Seismol Res Lett. 2020; 91(1): 272-86. https://doi.org/10.1785/0220190180

[77] Çakir Ö, Kutlu YA. A new method for selecting the phase and group velocity dispersion curves of rayleigh and love surface waves: real data case of central Anatolia, Turkey (Türkiye). Indones J Earth Sci. 2023; 3(2): A795. https://doi.org/10.52562/injoes.2023.795

[78] Seredkina AI. The state of the art in studying the deep structure of the earth's crust and upper mantle beneath the baikal rift from seismological data. Izvestiya Phys Solid Earth. 2021; 57(2): 180-202. https://doi.org/10.1134/S1069351321020117

[79] Cheng Z, Peng C, Chen M. Real-time seismic intensity measurements prediction for earthquake early warning: a systematic literature review. Sensors. 2023; 23(11): 5052. https://doi.org/10.3390/s23115052

[80] Hakim AR, Saputro AH, Rohadi S, Gunawan MT, Kardoso R. Seismic Noise Analysis in InaTEWS Earthquake Station Network (Case Study: Flores Earthquake 7.4, 14 December 2021). IOP Conf Ser Earth Environ Sci. 2022; 1047(1): 012019. https://doi.org/10.1088/1755-1315/1047/1/012019